Behavioral/Cognitive

Neural Control of Vascular Reactions: Impact of Emotion and Attention

Hadas Okon-Singer,[1,2,3] Jan Mehnert,[2,4,5] Jana Hoyer,[2] Lydia Hellrung,[2] Herma Lina Schaare,[2] Juergen Dukart,[2,6,7] and Arno Villringer[2,3,4]

[1]Department of Psychology, University of Haifa, 3498838 Haifa, Israel, [2]Department of Neurology, Max Planck Institute for Human Cognitive and Brain Sciences, 04103 Leipzig, Germany, [3]Mind Brain Institute at Berlin School of Mind and Brain, Humboldt-University, 10099 Berlin, Germany, [4]Charité University Hospital, 10117 Berlin, Germany, [5]Machine Learning Group, Berlin Institute of Technology, 10587 Berlin, Germany, [6]Laboratoire de Recherche en Neuroimagerie, Département des Neurosciences Cliniques, Centre Hospitalier Universitaire Vaudois, Université de Lausanne, 1011 Lausanne, Switzerland, and [7]F. Hoffmann-La Roche, pRED, Pharma Research and Early Development, DTA Neuroscience, 4070 Basel, Switzerland

This study investigated the neural regions involved in blood pressure reactions to negative stimuli and their possible modulation by attention. Twenty-four healthy human subjects (11 females; age = 24.75 ± 2.49 years) participated in an affective perceptual load task that manipulated attention to negative/neutral distractor pictures. fMRI data were collected simultaneously with continuous recording of peripheral arterial blood pressure. A parametric modulation analysis examined the impact of attention and emotion on the relation between neural activation and blood pressure reactivity during the task. When attention was available for processing the distractor pictures, negative pictures resulted in behavioral interference, neural activation in brain regions previously related to emotion, a transient decrease of blood pressure, and a positive correlation between blood pressure response and activation in a network including prefrontal and parietal regions, the amygdala, caudate, and mid-brain. These effects were modulated by attention; behavioral and neural responses to highly negative distractor pictures (compared with neutral pictures) were smaller or diminished, as was the negative blood pressure response when the central task involved high perceptual load. Furthermore, comparing high and low load revealed enhanced activation in frontoparietal regions implicated in attention control. Our results fit theories emphasizing the role of attention in the control of behavioral and neural reactions to irrelevant emotional distracting information. Our findings furthermore extend the function of attention to the control of autonomous reactions associated with negative emotions by showing altered blood pressure reactions to emotional stimuli, the latter being of potential clinical relevance.

Introduction

Threatening stimuli prototypically facilitate adaptive motor behavior and activate the autonomic nervous system, affecting heart rate and blood pressure (Lang et al., 2000). These vascular responses can aggravate when the threatening situation develops into stress for the organism. It has been shown that, among healthy subjects, those with higher blood pressure responses are more likely to subsequently develop hypertension (Matthews et al., 2004). It is therefore highly relevant to identify neural mechanisms for the vascular response and potential ways to modulate it.

Studies on the neural underpinnings of vascular response to stress identified brain areas known to be associated with emotion processing, including the amygdala, insula, and cingulate (Gianaros and Sheu, 2009). These pioneer studies used intermittent blood pressure measurements between functional neuroimaging and were therefore limited to longer-lasting "stress periods." Recent technical developments (Gray et al., 2009), however, on which we build here, allow for simultaneous recording of blood pressure during fMRI to match neural activity associated with brief (threatening) events closely to blood pressure changes.

Regarding potential ways to modulate emotion-related autonomic responses, a crucial question concerns the degree to which reactions to emotional stimuli are affected by cognitive mechanisms. A debate exists on whether processing of emotional items depends on allocation of sufficient attention to them (see Pessoa et al., 2002 and Evans et al., 2011 for similar effects on attention bias to drug-related cues in drug-addicts). Recent models propose that projections from frontoparietal regions to amygdala modulate reactions to emotional stimuli (cf. Pessoa, 2009, Pourtois et al., 2013). Conversely, it has been suggested that although attention influences emotion processing, it may not affect neural activation related to defensive motor responses (Pichon et al., 2012). If the latter were coupled to autonomic responses, this would mean that (action-related) vascular responses to emotional stimuli could occur independently of attention to them.

Motivated by these considerations, the aims of this study were to identify neural regions involved in blood pressure responses to emo-

Received Feb. 18, 2013; revised Jan. 12, 2014; accepted Jan. 20, 2014.

Author contributions: H.O.-S., J.H., and A.V. designed research; H.O.-S. performed research; J.M., L.H., and J.D. contributed unpublished reagents/analytic tools; H.O.-S., J.M., and L.S. analyzed data; H.O.-S., J.M., J.H., L.H., L.S., J.D., and A.V. wrote the paper.

We thank Bettina Johst, Andre Pampel, and Jöran Lepsien for technical support; Heike Schmidt and Stephan Liebig for help with the graphics; and Noga Cohen for helpful comments on previous versions of this manuscript.

The authors declare no competing financial interests.

Correspondence should be addressed to Hadas Okon-Singer, University of Haifa, Mount Carmel, 3498838 Haifa, Israel. E-mail: hadasos@psy.haifa.ac.il.

DOI:10.1523/JNEUROSCI.0747-13.2014

 0270-6474/14/344251-09$15.00/0

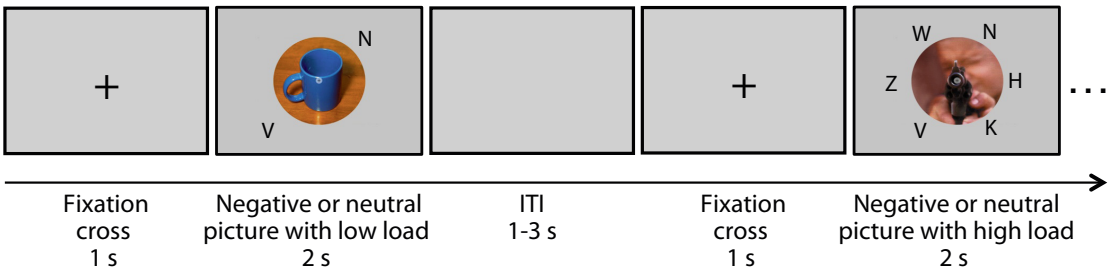

Figure 1. Examples of low-load and high-load trials. In each trial, a fixation cross was presented for 1 s, followed by presentation of a target letter (i.e., "X" or "N") with either one (i.e., low load) or five (i.e., high load) distracting letters. Simultaneously to the letters, a distracting picture, either neutral or negative, appeared. The valence of the picture was independent of the load condition. ITI, Intertrial interval.

tional stimuli and to elucidate whether and how attention modulates these neural processes and the associated vascular response.

Our study builds on an affective perceptual load task that we previously established to assess the impact of attention on emotion processing (Okon-Singer et al., 2007). Participants discriminate a target letter among few (low load) or many (high load) distractor letters, whereas they are asked to ignore simultaneously presented distractor pictures that are emotionally negative or neutral. Using this paradigm, we investigated whether attention affects behavioral, neural, and vascular reactions to irrelevant emotional distractors in healthy individuals. In the low-load condition, negative pictures were hypothesized to deteriorate task performance, to activate regions implicated in emotion processing (amygdala, anterior insula, orbitofrontal cortex, visual areas), and to transiently decrease blood pressure (Minati et al., 2009, Dan-Glauser and Gross, 2011). In high load (reduced attention) these reactions were hypothesized to be attenuated. Finally, we expected activations related to enhanced perceptual load in frontoparietal and primary visual regions.

Materials and Methods

Subjects

Twenty-four healthy subjects (11 females; mean age = 24.75 ± 2.49 years) without any history of neurological, psychiatric, vascular, or cardiologic diseases volunteered to participate in the study in return for payment. The study was approved by the local ethics committee and all subjects gave informed consent before the experiment. All subjects were right handed according to the Edinburgh Handedness Inventory (Oldfield, 1971) and all fell in the normal range of anxiety and stress as assessed by the German version of the Spielberger State-Trait Anxiety Inventory (Laux et al., 1981) and the Trier Inventory of Chronic Stress (Schulz and Schlotz, 1999), respectively.

Due to technical problems, the behavioral data of five subjects was not recorded, so the behavioral analysis is based on 19 subjects (11 females). In addition, after technical challenges involved in recording blood pressure continuously and noninvasively inside the MRI scanner, the blood pressure measurement of eight of the initial 24 subjects contained >40% signal dropout (caused by slight movements of the subjects resulting in signal loss and low-pressured attachment of blood pressure sensors; see further details regarding data preprocessing in the "Blood pressure preprocessing" section). Therefore, we performed two types of analyses (see details in "Data analysis" below): (1) analysis of the fMRI data, without correlating them to the blood pressure measures, was performed to examine the neural correlates of the interaction between attention and emotion and was based on fMRI data acquired from all 24 participants (the fMRI data were not affected by the signal dropouts); and (2) analyses correlating the fMRI data with the blood pressure measurements, which had to be conducted based on 16 participants (nine females) due to the signal dropouts and unreliable blood pressure data from eight subjects and include both a parametric modulation analysis and an analysis with a continuous blood pressure regressor (see details in the "Correlation with blood pressure: parametric modulation analysis" and the "Correlation with continuous blood pressure" sections).

Stimuli and design

Stimuli pictures (distractors) were modified, color real-life photos from the International Affective Picture System (IAPS; Lang et al., 2008). To avoid differences in complexity between the pictures, we modified the original IAPS pictures using clipping and, where necessary, magnification. The emotional valence and arousal levels of the modified pictures were judged by a sample of 41 (20 males, mean age = 26.0 ± 4.6 years) healthy volunteers. For the current experiment, 80 negative and 80 neutral pictures were chosen based on the valence scores of the modified pictures. We did not examine possible differences in the blood pressure response to subtypes of pictures, such as aggressive compared with disgusting images. Visual features were further matched between negative and neutral pictures. *t* tests showed no difference in luminance, contrast, or dominant spatial frequency between the negative and the neutral pictures (all *t*-values <0.53, all *p*-values >0.6). Furthermore, the content of the pictures (i.e., people, objects, or scenes) was similar across conditions.

Figure 1 describes the order of events in an experimental trial. Each trial started with a fixation cross shown for 1 s, followed by a negative or a neutral picture in the center of the screen for 2 s. The picture was presented as a circular shape and was surrounded by either two (i.e., low perceptual load; 50% of the trials) or six (i.e., high perceptual load) letters presented in an imaginary circle. The letters always included a target letter (i.e., "X" or "N") and one or five distracting letters. Participants were asked to ignore the picture and discriminate the target letter. They were asked to press different buttons in the response box allocated to indicate either "X" or "N" using the index and middle finger of their right (dominant) hand. They were requested to respond as fast and accurately as possible. Before the fMRI session, subjects performed a short practice session outside the scanner to familiarize them with the task. The experiment was presented in short blocks separated by "null trials" to control for habituation and expectancy effects. The trials were presented in a pseudorandomized order, with the criteria that no more than three consecutive short blocks of the same emotional valence (i.e., negative or neutral) were presented. The reason for using a block design was to maximize the vascular reactivity and neural reactions to the task. Block designs are known to produce more robust effects in fMRI compared with event-related designs (Friston et al., 1999).

Data acquisition

fMRI acquisition. fMRI acquisition was performed on a 3T scanner (Siemens). All images were acquired using a 12-channel head coil. Functional images were acquired using a gradient-echo EPI sequence (FOV 19.2 cm, matrix size 64 × 64, voxel size 3 × 3 × 4 mm^3, TR/TE/FA = 2000/30/90, 30 axial slices of 3 mm with an interslice gap of 1 mm). Anatomical scans were acquired in a separate session using a T1-weighted 3D MP-RAGE sequence (FOV 256 × 240 mm^2, spatial resolution 1 × 1 × 1.5 mm^3). Geometric distortions were characterized by a B0 field-map scan. The field-map scan consisted of gradient-echo readout (24 echoes, inter-TE 0.95 ms) with a standard 2D phase encoding. The B0

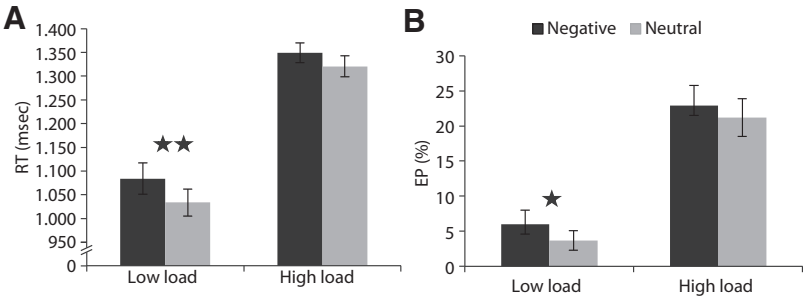

Figure 2. Analysis of RT and EP in the perceptual load task revealed that in the low-load condition, negative distractor pictures resulted in longer RT (***A***) and reduced accuracy (***B***) compared with neutral distractor pictures. In the high-load condition, these differences were not significant. Error bars indicate SD.

Table 1. RT and EP analysis in the perceptual load task

	Mean	SD	*t* test	*p*-value
RT (msec)				
Low load				
Negative	1083.9	33.1	2.96	0.008
Neutral	1033.59	28.5		
High load				
Negative	1349.1	21.1	1.17	0.25
Neutral	1320.4	22.2		
EP (error %)				
Low load				
Negative	6.0	2.0	2.37	0.029
Neutral	3.7	1.4		
High load				
Negative	22.9	2.9	0.9	0.37
Neutral	21.2	2.7		

In the low-load condition, negative distractor pictures resulted in slower RT and higher EP compared with neutral distractor pictures. These differences were not significant in the high-load condition.

Table 2. Blood pressure reaction in response to distractor pictures and different load conditions in the perceptual load task

	Mean	SD	*F* test	*p*-value
Low load				
Negative	−0.48	1.29	4.34	0.055
Neutral	0.403	1.66		
High load				
Negative	−0.12	1.71	1.59	0.22
Neutral	−0.78	1.35		

In the low-load condition, blood pressure was lower after negative compared with neutral distractor pictures. The difference between negative and neutral distractor pictures was not significant in the high-load condition. Blood pressure changes are reported as a change from mean baseline from 1 s before the beginning of each block to the onset of the first picture in the block.

field was obtained by a linear fit to the unwrapped phases of all odd echoes.

Blood pressure acquisition. Blood pressure was continuously recorded simultaneously to fMRI acquisition using an MR-compatible biophysical measurement system (CareTaker unit; Empirical Technologies/Biopac Systems; http://www.biopac.com/). Given the high correlation between their time courses ($r = 0.9219$), further analyses were conducted only on systolic blood pressure because systolic blood pressure has been shown to have higher reactivity to stress (Krantz and Manuck, 1984; Sherwood et al., 1990; Swain and Suls, 1996) and other stimuli (Gravlee and Brockschmidt, 1990) compared with diastolic blood pressure.

An arterial pulse signal was measured noninvasively via a small plastic device that was sensitive to pressure and attached firmly to the L brachial artery. The signal was transformed in real-time to systolic and diastolic blood pressure values using a Pulse Decomposition Analysis (PDA) algorithm (Baruch et al., 2007; Baruch et al., 2011). In short, the PDA algorithm uses the temporal structure of the pressure pulse to extract features highly correlated with diastolic and systolic blood pressure. The assumption is that the pressure pulse consists of a main, leading pressure component and two following components rising from reflections of the first one. The temporal delay between the first and the third pressure component in combination with their amplitudes are thereby highly correlated with systolic and diastolic blood pressure. Notably, the algorithm calculates neither diastolic nor systolic blood pressure from the mean arterial pressure.

After calibration with individual blood pressure readings from a blood pressure cuff (Biopac Systems), the pulse decomposition analysis algorithm was used to track blood pressure by analyzing the timing and amplitudes of the primary L ventricular ejection pulse and arterial pulse reflections in the upper arm. To avoid movement artifacts, subjects responded to the task using the index and middle fingers of their right hand while the blood pressure device was attached to their left arm. To ensure subject safety, only plastic MR-compatible parts of the system entered the scanner room and the data were transferred using a transducer, Bluetooth dongle, USB D/A converter and cables, and an INISO optically isolated input adapter. Data were sampled at a 500 Hz sampling rate. To maintain sufficient pressure, an automatic blood pressure calibration unit was used and, if necessary, air was pumped into the plastic device attached to the subjects (e.g., in instances in which small movements of the subject affected the blood pressure pad connection to the artery). The data were acquired via the CareTaker blood pressure software module and transferred to AcqKnowledge software (BioPac Systems), which also saved triggers at the onset of each picture onset to allow for the synchronization with the fMRI data.

Data preprocessing

fMRI preprocessing. Functional data were processed and analyzed using Statistical Parametric Mapping software (SPM8; Wellcome Department of Imaging Neuroscience, London, United Kingdom) with MATLAB 7.11.0 software (MathWorks). Preprocessing included the following steps: removal of the first 10 s (first five repetitions) to achieve a scanner steady state, motion correction using realignment to the first volume, geometric distortions correction using a field map, and slice timing correction to the middle slice. Functional and anatomical images were normalized to Montreal Neurological Institute (MNI) space. Images were then spatially smoothed with an 8 mm full-width at half-maximum Gaussian kernel and a high-pass filter of 1/128 Hz was applied.

Blood pressure preprocessing. The systolic blood pressure raw data were corrected for clearly visible artifacts (when pressure went below 3 SDs from its mean) using a linear interpolation between the last corrected blood pressure value before the artifacts occurrence and the first value afterward. Subjects for whom >40% of the data had to be interpolated were excluded from any further analysis, resulting in 16 subjects being used for analyses of blood pressure data. Within these 16 subjects, 3.1% (SD = 5.9%) of the data were interpolated (25.3/0.3 max/min in individuals). For the parametric modulation analysis, we calculated one value for systolic blood pressure in each block. These values were based on an average of the values from 3 s after the first picture onset in a block to 5 s after the end of the block (based on Gray et al., 2009 and James et al., 2013) minus a baseline based on the values of the second before the block onset (i.e., period of −1 to zero when zero is the first stimulus onset in a block). These values were used in the analysis of the blood pressure responses and for the parametric analysis with the fMRI data. For the analyses of the relation of neural activation to blood pressure fluctuations, we prepared a continuous regressor for systolic pressure that was based on one blood pressure value for each TR.

Data analysis

Behavioral data analysis. The analyses of behavioral data included reaction time (RT) and accuracy (error percentage; EP) and was performed

Table 3. Brain regions activated during the perceptual load task

Side	Region	MNI coordinates			*t*-value	Voxels
		x	*y*	*z*		
Regions that exhibited enhanced activation for negative vs neutral pictures						
R	Middle frontal gyrus	42	5	34	5.58	21
R	Inferior frontal gyrus	48	20	22	5.49	24
R	Inferior frontal gyrus	51	32	4	5.77	44
L	Superior frontal gyrus	−3	53	28	5.20	8
L	Inferior frontal gyrus	−36	23	1	6.53	106
L	Orbito-frontal cortex	−27	17	−17	5.40	10
R	Lateral occipital cortex	51	−70	7	9.89	681
L	Fusiform gyrus	−39	−49	−17	7.94	603
R	Amygdala	21	−4	−14	5.70	13
L	Amygdala	−21	−4	−14	5.75	24
R	Brainstem	9	−28	−8	5.53	11
R	Cerebellum	21	−76	−44	5.10	5
L	Cerebellum	−18	−76	−41	6.50	50
Regions that exhibited enhanced activation for neutral vs negative pictures						
R	Temporal lobe/lateral ventricle	18	−37	13	5.58	7
L	Temporal lobe	−27	−46	1	5.38	9
Regions that exhibited enhanced activation in the low-load vs the high-load condition						
	Medial frontal gyrus	0	47	−20	5.43	35
L	Superior medial frontal gyrus	−9	56	28	5.30	11
R	Middle temporal gyrus	57	−64	−5	7.02	64
R	Middle occipital gyrus	27	−94	−2	5.42	14
R	Hippocampus	21	−7	−17	5.13	5
L	Hippocampus	−24	−13	−17	5.94	47
Regions that exhibited enhanced activation in the high-load vs the low-load condition						
R	Middle frontal gyrus	33	47	19	7.75	180
L	Middle frontal gyrus	−33	50	13	6.43	47
L	Middle frontal gyrus	−24	2	49	5.61	20
R	Inferior frontal gyrus	30	26	−5	7.41	122
R	Supplementary motor area	18	11	64	5.38	8
L	Supplementary motor area	−9	14	46	6.11	87
R	Inferior parietal lobule	42	−52	49	5.71	121
L	Superior parietal gyrus	−24	−61	49	7.34	309
L	Lingual gyrus	−9	−79	−5	10.54	1449
L	Insula/Inferior frontal gyrus	−33	20	−2	6.71	82
Regions that exhibited enhanced activation for negative vs neutral pictures in the low-load condition						
R	Inferior frontal/orbitofrontal gyrus	36	29	−11	4.97	6
R	Middle temporal gyrus	51	−70	7	8.16	217
L	Middle temporal gyrus	−48	−61	4	6.32	210
R	Inferior temporal gyrus	42	−40	−14	6.54	69
L	Fusiform gyrus	−39	−49	−17	5.27	11
L	Insula	−36	23	1	5.95	35
L	Cerebellum	−18	−76	−41	5.33	8
Similar contrast: amygdala examination using a small volume correction ($p < 0.05$ FWE corrected)						
R	Amygdala	18	−4	−11	4.30	58
L	Amygdala	−18	−7	−14	4.69	70
Regions that exhibited enhanced activation for neutral vs negative pictures in the low-load condition						
R	Caudate	21	−34	13	5.67	13
Regions that exhibited enhanced activation for negative vs neutral pictures in the high-load condition						
R	Fusiform gyrus	39	−49	−20	5.87	47
L	Fusiform gyrus	−39	−49	−17	5.46	27
R	Middle occipital gyrus	51	−73	1	5.73	16
L	Middle occipital gyrus	−42	−79	−2	5.11	7
No regions exhibited enhanced activation for neutral vs negative pictures in the high-load condition						

The table shows left (L) and right (R) regions that were activated in the corresponding analyses. For each region, the *t*-values for voxels of peak activation and their corresponding cluster sizes were derived from a whole-brain group analysis (see text for details). The table includes only clusters of at least five voxels.

using SPSS (version 18, http://www-01.ibm.com/software/analytics/spss/). For the RT analysis, only correct responses were included. Extreme responses (i.e., >3 SDs from the mean of the specific condition) were excluded. Mean RTs and EP data were used in a two-way factorial ANOVA with the factors valence (negative/neutral pictures) and load (low/high) as within-subjects effects.

Blood pressure responses. Similar to the analysis of the behavioral data, the analysis of the blood pressure responses was also performed using SPSS (version 18, http://www-01.ibm.com/software/analytics/spss/). As described above, for each subject, we calculated one value for systolic blood pressure in each block. These values were used in a two-way factorial ANOVA with the factors valence (negative/neutral pictures) and load (low/high) as within-subjects effects.

fMRI analysis of the task conditions. To examine the effect of the task on neural activation, whole-brain voxelwise general linear model analyses were conducted on the first level. The analysis was based on a block design similar to the analyses of the behavioral performance and the blood pressure reaction. Regressors modeling stimulus events were locked to the first stimulus onset in each experimental block and convolved with a canonical hemodynamic response function (HRF). The

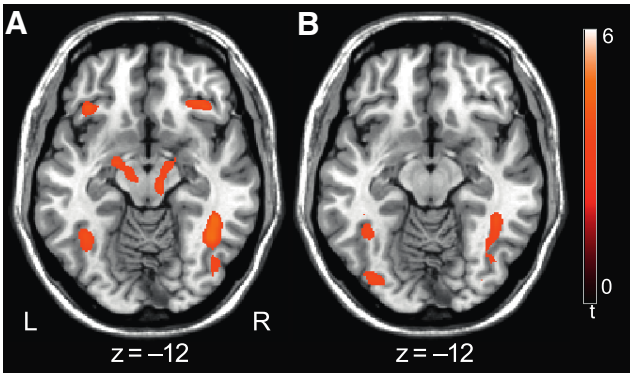

Figure 3. Neural regions that revealed enhanced activation in the perceptual load task when contrasting negative (in red) and neutral (in blue) distractor pictures in the low-load (***A***) and high-load (***B***) conditions. Results were thresholded at $p < 0.05$ FWE corrected.

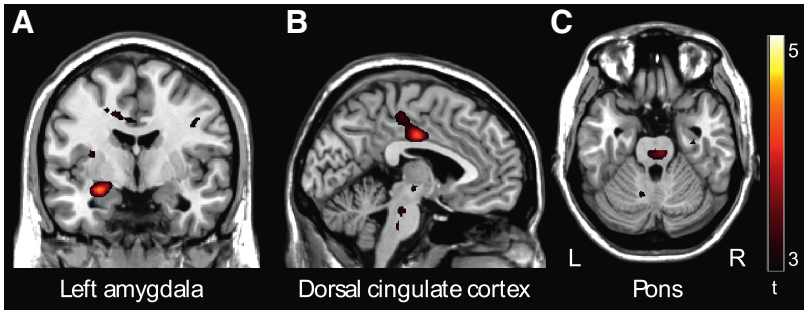

Figure 4. Neural regions that revealed enhanced positive correlation with changes in blood pressure in the low-load condition when contrasting negative and neutral pictures. Results were thresholded at $p < 0.001$ uncorrected. ***A***, Coronal section. ***B***, Sagittal section. ***C***, Horizontal section.

analysis model included the task conditions and six motion realignment nuisance regressors. A factorial design was applied with emotion (negative/neutral) and load (low/high) as within-subjects factors. The individual maps of activation were entered into a group analysis computed with random effects controlling for voxelwise multiple comparisons using a familywise error rate (FWE) threshold of $p < 0.05$ (Friston et al., 1996). In addition, based on our hypothesis that the amygdala would be involved in the reaction to emotional stimuli, we specifically analyzed this region as a region of interest (ROI). The coordinates for the amygdala analysis were based on a recent meta-analysis of reactions to emotional items (amygdala left: −20, −6, −17; right: 22, −3, −17; Sabatinelli et al., 2011). Considering the small size of the amygdala (1500 mm^3; Amunts et al., 2005), we used a small volume correction using 8-mm-radius sphere based on a formula for radius calculation for a spherical shape. Subjects were included as a between-subjects factor to correct for individual differences in activation. The group level model further included a nuisance regressor of sex (Sacher et al., 2012). To examine early and later effects of attention on the reaction to the emotional distractors, we further plotted the time course of regions that were related to the task's reactions. Coordinates for the ROIs were chosen based on Table 3. We examined regions that are important based on previous literature related to emotional processing and/or emotion control (Sabatinelli et al., 2011). We chose cortical and subcortical regions to investigate the potential differences in their time courses. Therefore, the following regions were chosen: bilateral amygdala, L middle frontal gyrus, and right inferior frontal gyrus. To avoid overlapping responses between trials, the time courses are based on averages of the first trial in each experimental block. Analyses were performed using rfxplot toolbox for SPM using the Peri-Stimulus Time Histogram option (Gläscher, 2009).

Correlation with blood pressure: parametric modulation analysis. To examine possible differences between the task conditions in the activation of neural regions that are related to systolic blood pressure, we conducted a parametric modulation analysis model in SPM. On the individual level, the statistical model included the task conditions as regressors (as mentioned in fMRI analysis of the task conditions, above), a blood pressure parameter for each condition and experimental block, and the six movement realignment parameters. Contrast maps were computed on the first level for each parameter (i.e., negative/neutral pictures × low/high load). These contrast maps were entered in factorial analysis on the group level, with a general factor of subjects and sex as a covariate, similarly to previous analyses described above (see "fMRI analysis of the task conditions" section). An analysis based on a FWE-corrected p-value yielded very few regions of activation, probably due to the relatively low number of remaining subjects after excluding subjects with many signal dropouts. Therefore, we report results based on a p-value of 0.001.

Correlation with continuous blood pressure. To examine possible relation between neural activation of and blood pressure fluctuations, we conducted an analysis with a continuous blood pressure regressor in SPM. Similarly to the other analyses, we focused on systolic blood pressure. The individual-level statistical model included the systolic blood pressure continuous regress, the task regressor, and six motion realignment parameters as covariates of no-interest. A regression analysis at the first level was followed by a one-sample t test at the group level computed with random effects modeling sex as a covariate of no-interest, similarly to previous analyses described above (see "fMRI analysis of the task conditions" section). Similarly to the parametric modulation analysis, we report results based on a p-value of 0.001.

Results

Behavioral performance

Separate analyses were performed for RT and EP. The ANOVA revealed a main effect of valence due to longer RTs after presentation of negative pictures compared with neutral pictures ($F_{(1,18)} = 5.12$, $p = 0.03$). The same trend in EP did not reach significance ($F_{(1,18)} = 2.93$, $p = 0.1$). In addition, RTs were longer and EP was higher in the high-load compared with the low-load condition ($F_{(1,18)} = 172.7$, $p = 0.001$ and $F_{(1,18)} = 90.6$, $p = 0.001$ for RT and EP, respectively). The interaction between load and valence was not significant ($F_{(1,18)} = 1.39$, $p = 0.25$ and $F_{(1,18)} = 0.08$, $p = 0.7$ for RT and EP, respectively). However, based on our a priori hypotheses, we further examined the difference between negative and neutral picture trials in the low-load and high-load conditions separately. As expected, the difference between negative and neutral pictures was significant in the low-load condition ($t_{18} = 2.96$, $p = 0.008$ and $t_{18} = 2.37$, $p = 0.029$, for RT and EP, respectively). In the high-load condition, the difference between negative and neutral pictures was not significant ($t_{18} = 1.17$, $p = 0.25$ and $t_{18} = 0.9$, $p = 0.37$, for RT and EP, respectively; Fig. 2, Table 1).

Blood pressure responses

An ANOVA revealed an interaction between load and valence ($F_{(1,15)} = 7.35$, $p = 0.01$). *Post hoc* analyses revealed that this interaction resulted from an opposite pattern between low and high load: in the low load, systolic blood pressure responses were lower when negative pictures were presented, compared with neutral pictures ($F_{(1,15)} = 4.34$, $p = 0.055$). In contrast, in the high-load condition, systolic blood pressure responses did not differ significantly between negative and neutral pictures ($F_{(1,15)} = 1.59$, $p = 0.22$; Table 2). The main effects of load and valence were not significant (all $f < 1.08$; all $p > 0.3$).

Table 4. Brain regions activated during the perceptual load task in correlation with blood pressure changes

Side	Region	MNI coordinates			*t*-value	Voxels
		x	*y*	*z*		
Regions that exhibited enhanced correlation with blood pressure for negative vs neutral pictures ($p < 0.001$ uncorrected)						
L	Supplementary motor area	−9	−22	49	3.72	11
L	Postcentral gyrus	−21	−40	70	4.16	12
L	Middle temporal cortex	−42	−7	−20	3.60	6
L	Insula/caudate	−33	−37	22	4.04	7
L	Amygdala	−27	−4	−17	3.56	7
R	White matter	24	−16	37	3.91	19
No regions exhibited enhanced correlation with blood pressure for neutral vs negative pictures						
No regions exhibited enhanced correlation with blood pressure for the low-load vs the high-load condition						
Regions that exhibited enhanced correlation with blood pressure for the high-load vs the low-load condition						
R	Anterior cingulate cortex	18	38	16	4.41	79
L	Precentral gyrus	−54	2	28	3.31	8
L	Caudate	−24	14	22	3.30	5
L	White matter	−18	17	34	4.39	33
Regions that exhibited enhanced correlation with blood pressure for negative vs neutral pictures in the low-load condition						
R	Middle frontal gyrus	36	8	34	3.70	15
R	Lateral prefrontal cortex	42	23	40	3.57	5
L	Lateral prefrontal cortex	−42	47	16	3.47	6
R	Inferior frontal gyrus/Insula	54	26	1	3.70	6
L	Supplementary motor area	−9	−22	49	3.79	13
R	Dorsal cingulate	21	−16	40	5.20	374
R	Posterior cingulate	21	−46	34	4.75	61
L	Superior parietal gyrus	−18	−40	70	3.99	12
L	Superior parietal gyrus	−27	−43	64	3.60	5
L	Inferior parietal cortex	−57	−46	37	3.51	17
L	Inferior parietal cortex	−42	−58	37	3.55	16
L	Insula	−39	−22	10	4.09	45
R	Parahippocampal gyrus	30	−19	−20	4.11	29
L	Amygdala	−27	−4	−14	4.57	
R	Putamen	21	8	−11	3.62	9
L	Putamen	−30	5	−11	4.68	86
R	Midbrain	9	−10	−8	4.48	28
R	Midbrain	6	−25	−26	3.78	21
R	Cerebellum	33	−76	−38	3.97	17
No regions exhibited enhanced correlation with blood pressure for neutral vs negative pictures in the low-load condition. In the high-load condition, no regions exhibited enhanced correlation with blood pressure either for negative vs neutral pictures or for neutral vs negative pictures						
Regions that exhibited a correlation with continuous blood pressure						
R	Superior frontal gyrus	18	14	46	4.90	13
R	Frontal pole	27	65	19	4.57	10
L	Frontal pole	−39	56	10	5.12	13
L	Frontal pole	−6	68	16	4.28	5
L	Prefrontal cortex (bilateral)	−6	−7	67	7.12	352
L	Precentral gyrus	−21	−25	55	5.65	126
L	Cingulate gyrus	−6	−4	46	4.40	19
R	Parietal cortex	42	−49	31	4.13	5
R	Hippocampus	36	−19	−14	4.47	10
L	Cerebellum	−21	−31	−29	4.92	5
L	Cerebellum	−9	−55	−50	7.03	71
R	Cerebellum	9	−58	−50	5.47	14

Table shows left (L) and right (R) regions that were activated in the corresponding analyses. For each region, the *t*-values for voxels of peak activation and their corresponding cluster sizes were derived from a whole-brain group analysis (see text for details). The table includes only clusters of at least five voxels.

Neural responses to the task

Table 3 depicts the brain regions that were found in the whole brain analysis ($p < 0.05$, FWE corrected) of the perceptual load task when contrasting load, valence, and their interaction. In relation to our main hypothesis regarding attention, in the low-load condition, higher activation was revealed after negative pictures compared with after neutral pictures in the bilateral amygdala, the bilateral medial temporal cortex, the right inferior frontal cortex and the left insula: brain regions implicated in emotion processing. In the high-load condition, the difference between negative and neutral pictures was restricted to only a few vision brain regions (Fig. 3, Table 3).

Further examination of the time courses of several ROIs reveals clear differences between the amygdala and prefrontal regions (see Fig. 5). Although activation in bilateral amygdala was higher for negative compared with neutral distracting pictures, and in general higher in the low-load compared with the high-load condition, activation in prefrontal regions was higher during the high-load compared with the low-load condition. These activation patterns are consistent with the suggestion that attention resources had an impact on the neural response to distracting pictures. Additionally, they suggest that top-down control processes originating in frontoparietal regions might have affected the reduced neural responses during the high-

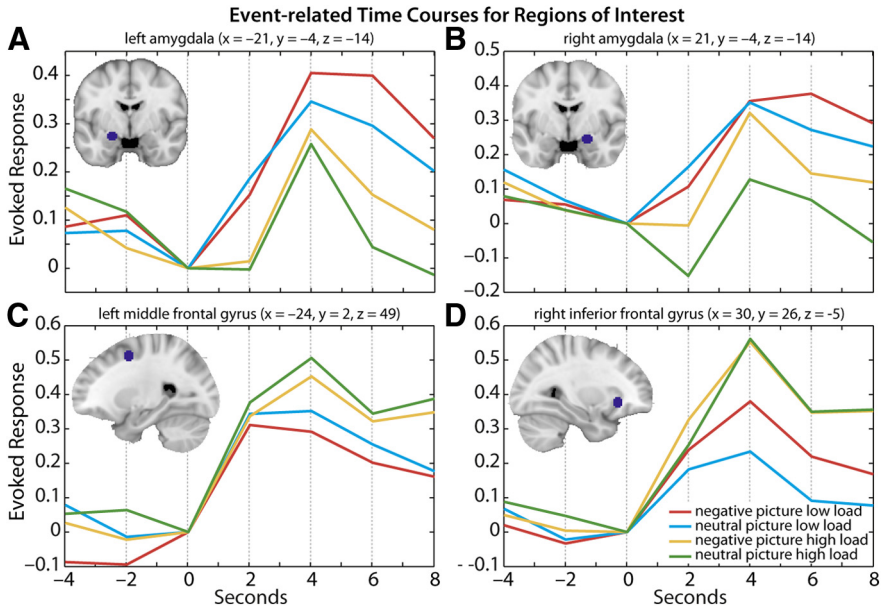

Figure 5. Time courses of fMRI-BOLD activations in the following ROIs: bilateral amygdala (***A***, ***B***), left middle frontal gyrus (***C***), and right inferior frontal gyrus (***D***). The plots are based on activation in a 6 mm sphere surrounding the coordinates. To avoid overlapping responses, the time courses are based on the first trials in the relevant block for each condition (see text for details).

load condition. Please note that our block design did not allow averaging of all the trials. Therefore, these time courses are based on an average of only the first trial in each block, yielding eight trials per condition for each subject. Furthermore, comparison of the timing between different regions is problematic because the HRF is known to differ between neural sites (Neumann et al., 2003).

Neural correlates of blood pressure: modulation by task conditions

Table 4 depicts the neural regions that correlated with changes in systolic blood pressure in the different task conditions. In the low-load condition, comparison of the neural regions related to systolic blood pressure responses to negative pictures compared with neutral pictures revealed activation in the bilateral lateral prefrontal cortex, the right dorsal and posterior cingulate, the left superior and inferior parietal cortex, the bilateral insula, the left amygdala, the bilateral putman, and the bilateral midbrain and cerebellar regions (Fig. 4, Table 4).

Neural correlates of blood pressure fluctuations

Table 4 shows the neural regions that positively correlated with changes in systolic blood pressure during the fMRI acquisition. This analysis revealed activation in bilateral frontal pole, bilateral prefrontal cortex, the right parietal cortex, the left cingulate cortex, the right hippocampus, and bilateral cerebellum.

Discussion

Using an affective perceptual load task, we found that in the low-load condition—when attention was available for processing distractor pictures—negative (compared with neutral) pictures deteriorated performance in the central task, activated brain regions known to be involved in emotion processing, and decreased blood pressure; we furthermore found a positive correlation between blood pressure response and activation in prefrontal and parietal regions, amygdala, caudate, and the midbrain. These effects were modulated by attention: behavioral and neural responses to highly negative distractor pictures were smaller or diminished, as was the negative blood pressure response when the central task involved high perceptual load. Furthermore, comparing the high-load and low-load conditions revealed enhanced activation in frontoparietal regions.

The finding of stronger behavioral interference of irrelevant pictures in the low-load condition confirms our previous results using the same task (Okon-Singer et al., 2007). The activation of amygdala, insula, orbitofrontal, visual, and cerebellar areas for negative pictures and the reduced activation in the high-load condition is also highly consistent with our hypothesis and previous findings. Subsequently, we discuss the results concerning the main aims of our study, the blood pressure response to emotion stimuli and the involved neural regions and the influence of attention on these responses. Finally, we speculate about clinical implications and suggest future studies.

Blood pressure response to emotional stimuli and involved brain areas

Emotions are strongly linked to physiological reactions via modulation of the autonomic system. Most previous fMRI investigations on neural correlates of blood pressure responses have either measured vascular responses at the end of stress-evoking blocks (Gianaros et al., 2006) or used replica protocols to correlate vascular responses measured outside the scanner with neural responses acquired with fMRI (Gianaros et al., 2012). Here, we measured blood pressure simultaneously to fMRI (pioneered by Gray et al., 2009) so the results represent neural and vascular responses to brief emotional stimuli. Furthermore, this design allows investigating the interaction between various mental processes occurring simultaneously. We cannot rule out possible influences of other factors, such as familiarity, and although we believe our results reflect neural activity that preceded vascular reactivity, it is possible that blood pressure responses themselves also influenced the measured neural activity.

Our finding of an early blood pressure decrease to negative stimuli is consistent with results showing heart rate deceleration and blood pressure decrease when viewing unpleasant pictures (Lang et al., 1993; Minati et al., 2009; Dan-Glauser and Gross, 2011; Wangelin et al., 2011). Blood pressure responses during emotional stimuli correlated with activity in bilateral lateral prefrontal cortex, the right dorsal and posterior cingulate cortex, the left insula, the left amygdala, midbrain, and cerebellar regions. These regions, which are known to be key players in emotion generation and regulation, are consistent with a meta-analysis of studies investigating neural correlates of vascular responses to stress (Gianaros and Sheu, 2009), and were shown to reduce the sensitivity of the arterial baroreflex during stress (Gianaros et al., 2012). Interestingly, these areas were related to blood pressure responses to emotional stimuli, but not to spontaneous fluctuations of blood pressure, pointing to recruitment of a neural network involved in vascular reactions associated with emotion.

Notably, BOLD signal in these areas correlated positively with blood pressure, which decreased with negative picture observa-

tion. Although we did not have the spatial resolution to parcel different amygdala subareas, it is tempting to speculate that different amygdala subareas are responsible for the blood pressure response and the overall response to negative pictures. Analogously, different amygdala subregions were shown to mediate valence-related and attention/predictiveness effects during emotional processing (Gamer et al., 2010; Boll et al., 2013).

Related to our study, there is recent work on neural correlates of peripheral autonomic activity in other settings: James et al. (2013) recorded muscle sympathetic nerve activity simultaneously to fMRI at rest. BOLD activity covaried with muscle sympathetic nerve activity in bilateral dorsolateral prefrontal cortex, precuneus, posterior cingulate cortex, hypothalamus, left insula, and left cerebellum (for review, see Macefield et al., 2013). Henderson et al. (2012) recorded skin sympathetic nerve activity simultaneously with fMRI during presentation of arousing pictures. Skin sympathetic nerve activity was positively related to activation in the right amygdala, bilateral thalamus, right nucleus accumbens, bilateral pons, and right cerebellum and negatively related to activation in the left orbitofrontal cortex, left frontal cortex, and right precuneus (see also Brown et al., 2012). Gray et al. (2009) measured cardiovascular responses to electric shocks administered at different time points of the cardiac rhythm simultaneously with fMRI. Their results imply that a network including the amygdala, insula, and brainstem is related to vascular reactions to painful stimuli. Although direct comparison between these studies and the current study is difficult due to methodological differences, we also found a relation to the amygdala only when examining blood pressure in response to the task and not during rest. All studies point to the involvement of frontal, limbic, midbrain, and cerebellar regions in the regulation of autonomous activity. Recent developments in autonomic signal acquisition simultaneously with fMRI may provide better differentiation of the neural networks regulating different autonomic systems in response to emotional stimulation and at rest.

Influence of attention on behavioral, neural, and blood pressure reaction to emotional stimuli

In our study, attention influenced behavioral and neural responses to negative pictures and there was an interaction between emotional valence and attention on the blood pressure response. Emotion theories typically consider both limbic-mediated projections to sensory areas related to the emotional salience of the stimulus and frontoparietal-mediated projections related to emotion regulation (Ochsner et al., 2012). Consistent with these models, we find modulation of neural responses due to the affective value of distracting pictures and allocation of attention. During low load, negative (compared with neutral) pictures led to higher activations in the amygdala, insula, orbitofrontal, visual, and cerebellar areas. These activations were reduced at high load. Furthermore, comparison of high and low load across picture types revealed enhanced activation in the middle and inferior frontal cortex, intraparietal lobule, and superior parietal lobule.

It is as yet unclear, however, whether these modulatory factors interact. Several studies support the notion that neural reactions to emotional stimuli depend on an interaction between "evaluative" and "control" projections (Pessoa et al., 2002; Van Dillen and Derks, 2012; for review, see Okon-Singer et al., 2012 and Iordan et al., 2013), but there are also conditions in which no interaction was found. For example, Gläscher et al. (2007) found attention and emotion not to interact; rather, their data indicated a "multiplicative gain effect of emotional salience." Additionally, in invasive amygdala recordings, there was an early attention-independent amygdala response preceding top-down attentional control effects (Pourtois et al., 2010; for review, see Pourtois et al., 2013). The 2 s picture presentation in our study would allow for both early control mechanisms and later top-down control; The frontoparietal activations that we found when comparing high and low load across picture types and the accordingly differential BOLD time courses given in Figure 5 suggest involvement of top-down cortical regions. Levens and Phelps (2010) showed that bilateral inferior frontal gyrus (found in our study when comparing high and low load across picture types) mediates interference resolution for both neutral and emotional items, whereas the left anterior insula and the right orbitofrontal cortex (found in our study when comparing negative and neutral distractors in low load) are specifically related to emotional distraction (see also Levens et al., 2011). Overall, we believe that at current levels of evidence, conclusions regarding the exact control mechanisms should be taken cautiously.

Implications, open questions, and perspectives

We believe that our approach provides a suitable setting for systematically studying the relationship among behavioral, neural, and physiological parameters during emotion processing. For example, it is not clear yet why the initial "negative" vascular response to emotional stimuli changes toward a later "positive" vascular response when threat continues (i.e., the "fight or flight" response). The underlying mechanisms are of potential clinical relevance because it has been shown that, among healthy, normotensive individuals, those in the upper quartile of blood pressure reaction to psychological stressors carry a higher risk of later developing hypertension (Matthews et al., 2004). In a similar vein, it has been suggested that "exaggerated" cardiovascular responses to stressors are mediated by abnormal brain structure, function, and connectivity (Gianaros et al., 2009a; Gianaros et al., 2009b) and that such neural abnormality may precede hypertension (Jennings and Zanstra, 2009). Our finding that attention modulates blood pressure response to emotional stimuli is consistent with the effect of emotion regulation on autonomic reactions (Dan-Glauser and Gross, 2011). These findings may provide a basis for preventive strategies for individuals at risk of developing hypertension. Further studies may elucidate neural factors predisposing individuals to vascular overreactions (i.e., at risk to develop hypertension) and enable the development of measures (e.g., emotion regulation, meditation) to prevent such vascular "overreactions."

References

Amunts K, Kedo O, Kindler M, Pieperhoff P, Mohlberg H, Shah NJ, Habel U, Schneider F, Zilles K (2005) Cytoarchitectonic mapping of the human amygdala, hippocampal region and entorhinal cortex: intersubject variability and probability maps. Anat Embryol (Berl) 210:343–352. CrossRef Medline

Baruch M, Kwon KW, Abdel-Rahman E, Isaacs R (2007) The structure of the radial pulse-a novel noninvasive ambulatory blood pressure device. Stud Health Technol Inform 125:40–42. Medline

Baruch MC, Warburton DE, Bredin SS, Cote A, Gerdt DW, Adkins CM (2011) Pulse decomposition analysis of the digital arterial pulse during hemorrhage simulation. Nonlinear Biomed Phys 5:1. CrossRef Medline

Boll S, Gamer M, Gluth S, Finsterbusch J, Büchel C (2013) Separate amygdala subregions signal surprise and predictiveness during associative fear learning in humans. Eur J Neurosci 37:758–767. CrossRef Medline

Brown R, James C, Henderson LA, Macefield VG (2012) Autonomic markers of emotional processing: skin sympathetic nerve activity in humans during exposure to emotionally charged images. Front Physiol 3:394. CrossRef Medline

Dan-Glauser ES, Gross JJ (2011) The temporal dynamics of two response-focused forms of emotion regulation: Experiential, expressive, and autonomic consequences. Psychophysiology 48:1309–1322. CrossRef Medline

Evans DE, Craig C, Oliver JA, Drobes DJ (2011) The smoking N-back: a measure of biased cue processing at varying levels of cognitive load. Nicotine Tob Res 13:88–93. CrossRef Medline

Friston KJ, Zarahn E, Josephs O, Henson RN, Dale AM (1999) Stochastic designs in event-related fMRI. Neuroimage 10:607–619. CrossRef Medline

Friston KJ, Holmes A, Poline JB, Price CJ, Frith CD (1996) Detecting activations in PET and fMRI: levels of inference and power. Neuroimage 4:223–235. CrossRef Medline

Gamer M, Zurowski B, Büchel C (2010) Different amygdala subregions mediate valence-related and attentional effects of oxytocin in humans. Proc Natl Acad Sci U S A 107:9400–9405. CrossRef Medline

Gianaros PJ, Sheu LK, Remo AM, Christie IC, Crtichley HD, Wang J (2009a) Heightened resting neural activity predicts exaggerated stressor-evoked blood pressure reactivity. Hypertension 53:819–825. CrossRef Medline

Gianaros PJ, Greer PJ, Ryan CM, Jennings JR (2006) Higher blood pressure predicts lower regional grey matter volume: Consequences on short-term information processing. Neuroimage 31:754–765. CrossRef

Gianaros PJ, Hariri AR, Sheu LK, Muldoon MF, Sutton-Tyrrell K, Manuck SB (2009b) Preclinical atherosclerosis covaries with individual differences in reactivity and functional connectivity of the amygdala. Biol Psychiatry 65:943–950. CrossRef Medline

Gianaros PJ, Sheu LK (2009) A review of neuroimaging studies of stressor-evoked blood pressure reactivity: emerging evidence for a brain-body pathway to coronary heart disease risk. Neuroimage 47:922–936. CrossRef Medline

Gianaros PJ, Onyewuenyi IC, Sheu LK, Christie IC, Critchley HD (2012) Brain systems for baroreflex suppression during stress in humans. Hum Brain Mapp 33:1700–1716. CrossRef Medline

Gläscher J (2009) Visualization of group inference data in functional neuroimaging. Neuroinformatics 7:73–82. CrossRef Medline

Gläscher J, Rose M, Büchel C (2007) Independent effects of emotion and working memory load on visual activation in the lateral occipital complex. J Neurosci 27:4366–4373. CrossRef Medline

Gravlee GP, Brockschmidt JK (1990) Accuracy of four indirect methods of blood pressure measurement, with hemodynamic correlations. J Clin Monit 6:284–298. CrossRef Medline

Gray MA, Rylander K, Harrison NA, Wallin BG, Critchley HD (2009) Following one's heart: Cardiac rhythms gate central initiation of sympathetic reflexes. J Neurosci 29:1817–1825. CrossRef Medline

Henderson LA, Stathis A, James C, Brown R, McDonald S, Macefield VG (2012) Real-time imaging of cortical areas involved in the generation of increases in skin sympathetic nerve activity when viewing emotionally charged images. Neuroimage 62:30–40. CrossRef Medline

Iordan AD, Dolcos S, Dolcos F (2013) Neural signatures of the response to emotional distraction: a review of evidence from brain imaging investigations. Front Hum Neurosci 7:200. CrossRef Medline

James C, Macefield VG, Henderson LA (2013) Real-time imaging of cortical and subcortical control of muscle sympathetic nerve activity in awake human subjects. Neuroimage 70:59–65. CrossRef Medline

Jennings JR, Zanstra Y (2009) Is the brain the essential in hypertension? Neuroimage 47:914–921. CrossRef Medline

Krantz DS, Manuck SB (1984) Acute psychophysiologic reactivity and risk of cardiovascular disease: a review and methodologic critique. Psychol Bull 96:435–464. CrossRef Medline

Lang PJ, Greenwald MK, Bradley MM, Hamm AO (1993) Looking at pictures–affective, facial, visceral, and behavioral reactions. Psychophysiology 30:261–273. CrossRef Medline

Lang PJ, Davis M, Ohman A (2000) Fear and anxiety: animal models and human cognitive psychophysiology. J Affect Disord 61:137–159. CrossRef Medline

Lang PJ, Bradley MM, Cuthbert BN (2008) International affective picture system (IAPS): affective ratings of pictures and instruction manual. Technical Report A-8. Gainesville, FL: University of Florida.

Laux L, Glanzmann P, Schaffner P, Spielberger CD (1981) Das State-Trait-Angstinventar. Theoretische Grundlagen und Handanweisung [in German]. Weinheim: Beltz Test.

Levens SM, Phelps EA (2010) Insula and orbital frontal cortex activity underlying emotion interference resolution in working memory. J Cogn Neurosci 22:2790–2803. CrossRef Medline

Levens SM, Devinsky O, Phelps EA (2011) Role of the left amygdala and right orbital frontal cortex in emotional interference resolution facilitation in working memory. Neuropsychologia 49:3201–3212. CrossRef Medline

Macefield, V.G., James, C., and Henderson, L (2013) Identification of sites of sympathetic outflow at rest and during emotional arousal: Concurrent recordings of sympathetic nerve activity and fMRI of the brain. Int J Psychophysiology.

Matthews KA, Katholi CR, McCreath H, Whooley MA, Williams DR, Zhu S, Markovitz JH (2004) Blood pressure reactivity to psychological stress predicts hypertension in the CARDIA study. Circulation 110:74–78. CrossRef Medline

Minati L, Jones CL, Gray MA, Medford N, Harrison NA, Critchley HD (2009) Emotional modulation of visual cortex activity: a functional near-infrared spectroscopy study. Neuroreport 20:1344–1350. CrossRef Medline

Neumann J, Lohmann G, Zysset S, von Cramon DY (2003) Within-subject variability of BOLD response dynamics. Neuroimage 19:784–796. CrossRef Medline

Ochsner KN, Silvers JA, Buhle JT (2012) Functional imaging studies of emotion regulation: a synthetic review and evolving model of the cognitive control of emotion. Ann N Y Acad Sci, 1251:E1–E24. CrossRef Medline

Okon-Singer H, Tzelgov J, Henik A (2007) Distinguishing between automaticity and attention in the processing of emotionally significant stimuli. Emotion 7:147–157. CrossRef Medline

Okon-Singer H, Lichtenstein-Vidne L, Cohen N (2013) Dynamic modulation of emotional processing. Biol Psychol 92:480–491. Medline

Oldfield RC (1971) The assessment and analysis of handedness: the Edinburgh inventory. Neuropsychologia 9:97–113. CrossRef Medline

Pessoa L (2009) How do emotion and motivation direct executive control? Trends Cogn Sci 13:160–166. CrossRef Medline

Pessoa L, McKenna M, Gutierrez E, Ungerleider LG (2002) Neural processing of emotional faces requires attention. Proc Natl Acad Sci U S A 99:11458–11463. CrossRef Medline

Pichon S, de Gelder B, Grèzes J (2012) Threat prompts defensive brain responses independently of attentional control. Cereb Cortex 22:274–285. CrossRef Medline

Pourtois G, Spinelli L, Seeck M, Vuilleumier P (2010) Temporal precedence of emotion over attention modulations in the lateral amygdala: Intracranial ERP evidence from a patient with temporal lobe epilepsy. Cogn Affect Behav Neurosci 10:83–93. CrossRef Medline

Pourtois G, Schettino A, Vuilleumier P (2013) Brain mechanisms for emotional influences on perception and attention: what is magic and what is not. Biol Psychol 92:492–512. CrossRef Medline

Sabatinelli D, Fortune EE, Li Q, Siddiqui A, Krafft C, Oliver WT, Beck S, Jeffries J (2011) Emotional perception: meta-analyses of face and natural scene processing. Neuroimage 54:2524–2533. CrossRef Medline

Sacher, J., Neumann, J., Okon-Singer, H., Gotowiec, S., and Villringer, A (2012) Sexual dimorphism in the human brain: evidence from neuroimaging. Magn Reson Imaging.

Schulz P, Schlotz W (1999) Das Trierer Inventar zur Erfassung von chronischem Streβ (TICS): Skalenkonstruktion, teststatistische Überprüfung und Validierung der Skala Arbeitsüberlastung [in German]. Diagnostica 45:8–19. CrossRef

Sherwood A, Dolan CA, Light KC (1990) Hemodynamics of blood pressure responses during active and passive coping. Psychophysiology 27:656–668. CrossRef Medline

Swain A, Suls J (1996) Reproducibility of blood pressure and heart rate reactivity: a meta-analysis. Psychophysiology 33:162–174. CrossRef Medline

Van Dillen LF, Derks B (2012) Working memory load reduces facilitated processing of threatening faces: an ERP study. Emotion 12:1340–1349. CrossRef Medline

Wangelin BC, Löw A, McTeague LM, Bradley MM, Lang PJ (2011) Aversive picture processing: effects of a concurrent task on sustained defensive system engagement. Psychophysiology 48:112–116. CrossRef Medline